

Recombination Parameters Measurement of Silicon Solar Cell Under Constant White Bias Light With Incident Angle

²Hamet Yoro BA, ³Boureima Seibou, ¹Idrissa GAYE, ²Ibrahima LY, ¹Gregoire SISSOKO
 (gsissoko@yahoo.com)

¹Laboratory of Semiconductors and Solar Energy, Physics Department, Faculty of Science and Technology - University Cheikh Anta Diop – Dakar – SENEGAL.

²Electromechanical Engineering Department, Polytechnic School of Thies – SENEGAL.

³School of Mines, Industry and Geology -Niamey NIGER

Abstract - The motivation of this work has been to extend the concept of junction and back surface recombination velocity S_f and S_b on a silicon solar cell under white bias illumination for minority carrier's recombination measurement and under various incident angle θ . The photocurrent density J_{ph} is presented as a calibrated function, diffusion length dependent, it intercepts with the experimental short circuit current density J_{SCexp} obtained from an automatic characterization device, at the effective minority carriers diffusion length L value. Also the intrinsic junction surface recombination velocity S_{f0} is determined from effective diffusion length.

Keywords - Silicon solar cell- recombination velocity- diffusion length-Incident angle.

INTRODUCTION

Many methods have been developed for determining lifetime, diffusion length and back surface recombination velocity of minority carriers in the base of solar cell. Steady methods, as photo response [1], were widely used for such parameters determination. The method could be subjected to limited wavelengths range condition [3]. Constant flux method as surface voltage [3] requires several assumptions which must be valid in order to measure the diffusion length. Transient methods [4-5], were performed and used either removable excitation (light or electrical) or removable charge under constant illumination. Impedance effects have been observed in solar cell response so that the electronic parameters deduced from the device could be strongly influenced.

Our main analysis is based on phenomenological parameters describing generation-diffusion and recombination processes that take place in solar cell under constant composite light illumination and for different incident angle values. A theoretical expression of the photocurrent density J_{ph} is presented as a calibrated function, diffusion length depending of incident angle values, it intercepts with the experimental short circuit current density J_{scexp} , at the effective minority carrier diffusion length L value. The effective diffusion length will be determined from photocurrent variation versus diffusion length. And the junction

intrinsic recombination velocity S_{f0} is obtained from L_{eff} .

The method proposed in this work considers the solar cell under a real operating condition, for various incident angle values [6-7-8].

I. THEORY

In this study, we use a silicon solar cell under a given incident angle θ .

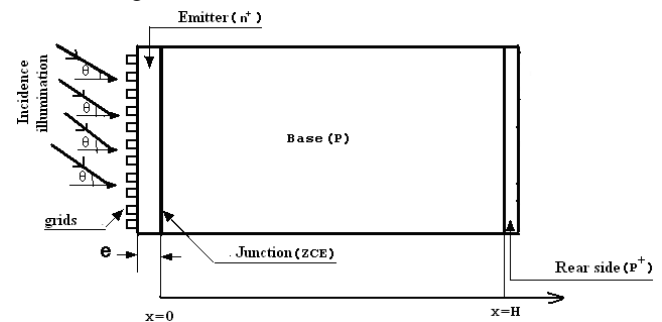


Figure1: schematic structure of a silicon solar cell

We consider a dominated base silicon solar cell n^+pp^+ [9]. The continuity equation for the excess minority carrier density $\delta(x)$ under steady state.

$$\frac{\partial^2 \delta(x)}{\partial x^2} - \frac{\delta(x)}{L^2} = -\frac{G(x)}{D} \quad (1)$$

Where D and L respectively are the minority carriers diffusion constant and diffusion length. The distance x is measured from the edge of the depletion layer in the base. The generation rate is expressed by the following relation:

$$G(x) = \cos(\theta) \sum_{i=1}^3 a_i \cdot e^{-b_i \cdot x} \quad (2)$$

Where a_i and b_i are coefficients from modeling of the generation rate over all the radiations in solar spectrum under A.M1.5.

Table1 : coefficients a_i and b_i values[11]

i	a_i	b_i
1	$6,13 \cdot 10^{20} \text{ cm}^{-3} \cdot \text{s}^{-1}$	6630 cm^{-1}
2	$0,54 \cdot 10^{20} \text{ cm}^{-3} \cdot \text{s}^{-1}$	10^3 cm^{-1}
3	$0,0991 \cdot 10^{20} \text{ cm}^{-3} \cdot \text{s}^{-1}$	130 cm^{-1}

Equation (1) is solved with following boundary conditions at the two edges:

- the junction interface at $x = 0$

$$\left. \frac{\partial \delta(x)}{\partial x} \right|_{x=0} = \frac{S_f}{D} \cdot \delta(0) \quad (3)$$

- the rear side at $x = H$

$$\left. \frac{\partial \delta(x)}{\partial x} \right|_{x=H} = -\frac{S_b}{D} \cdot \delta(H) \quad (4)$$

Where S_f and S_b are respectively the excess minority carriers' recombination velocities related to the back-surface and to the junction of the solar cell.

For the junction surface recombination velocity S_f , we have two terms: the intrinsic recombination velocity S_{f0} related to the junction and the recombination velocity S_f (load) imposed by the resistance load [3-10]. $S_f = S_{f0}(Le_{ff}) + S_f(\text{load})$

The steady state solution for minority carrier density can be expressed as.

$$\delta(x) = A \cdot \cosh\left(\frac{x}{L}\right) + B \cdot \sinh\left(\frac{x}{L}\right) - \frac{1}{D} \cdot \cos(\theta) \cdot \sum_{i=1}^3 a_i \cdot e^{-b_i \cdot H} \cdot \left(b_i^2 - \frac{1}{L^2}\right)^{-1} \quad (5)$$

Coefficients A and B can be determined through the boundary conditions.

On Figure 1, we give profile of minority carrier's density versus base depth for various incident angles in short circuit condition:

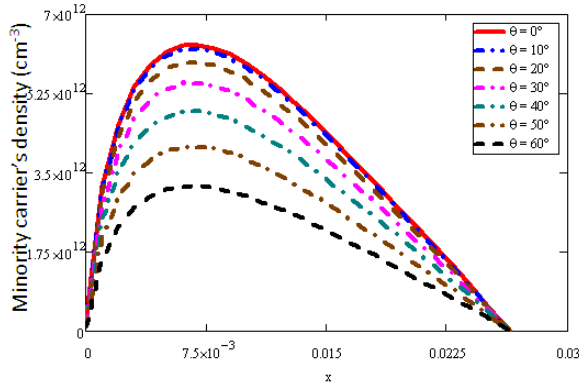


Figure 2: Excess minority carrier's density versus base depth

$$H = 0.03 \text{ cm } L = 0.01 \text{ cm}, S_f = 6.10^6 \text{ cm.s}^{-1} \text{ and } S_b = 3.10^3 \text{ cm.s}^{-1}$$

Figure 2 shows that pour chaque valeur de teta, la densité des porteurs diminue en profondeur dans la base.

II. PHOTOCURRENT

The photocurrent density expression is written as:

$$J_{ph} = q \cdot D \cdot \left. \frac{\partial \delta(x)}{\partial x} \right|_{x=0} \quad (6)$$

Replacing $\delta(x)$ in equation 6, we obtain the following expression:

$$J_{ph} = q \cdot \frac{D}{L} \cdot \cos(\theta) \cdot \sum_{i=1}^3 K_i \cdot S_f \cdot \frac{(b_i \cdot D - S_b) e^{-b_i \cdot H} + X - L b_i \cdot Y}{\frac{D}{L} \cdot X + S_f \cdot Y} \quad (7)$$

With

$$X = \frac{D}{L} \cdot \sinh\left(\frac{H}{L}\right) + S_b \cdot \cosh\left(\frac{H}{L}\right) \quad (8)$$

$$Y = \frac{D}{L} \cdot \cosh\left(\frac{H}{L}\right) + S_b \cdot \sinh\left(\frac{H}{L}\right) \quad (9)$$

We present in figure 3 the photocurrent density versus junction surface recombination velocity for different incident angle values [10-13-14].

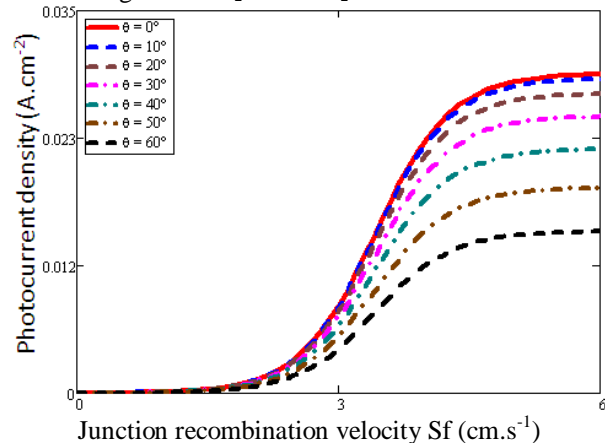


Figure 3: Photocurrent density versus Junction surface recombination velocity

$$H = 0.03 \text{ cm}, L = 0.01 \text{ cm}, S_b = 3.10^3 \text{ cm.s}^{-1}$$

For high S_f values, the photocurrent density J_{ph} is a horizontal line which gives the short circuit current density J_{sc} . For low S_f values, J_{ph} is zero and confirms that any charge carrier crosses the junction that corresponds to the open circuit condition.

II.1 Base recombination velocity

From figure 3, the photocurrent is constant for large S_f values, we then write:

$$\left[\frac{\partial J_{ph}}{\partial S_f} \right] = 0 \quad (10)$$

Solving equation (10) leads to the back surface recombination velocity expressed as diffusion length dependent.

$$S_b(L) = \frac{D}{L} \cdot \sum_{i=1}^3 \frac{L b_i \left(e^{-b_i \cdot H} - \cosh\left(\frac{H}{L}\right) \right) + \sinh\left(\frac{H}{L}\right)}{L b_i \cdot \sinh\left(\frac{H}{L}\right) - \cosh\left(\frac{H}{L}\right) + e^{-b_i \cdot H}} \quad (11)$$

Introducing $S_b(L)$ in the expression of the photocurrent density and taking S_f value very large, we obtain an expression of the short circuit current density both diffusion length and incident angle dependent, while optical (bi) and geometrical(H) parameters remained constant.

$$J_{sc}(L, \theta) = q \cdot \frac{D}{L} \cdot \cos(\theta) \sum_{i=1}^3 K_i \cdot \frac{(b_i \cdot D - S_b(L)) e^{-b_i \cdot H} + X - L b_i \cdot Y}{Y} \quad (12)$$

We present in figure 4 the short circuit current density versus diffusion length for different incident angle values.

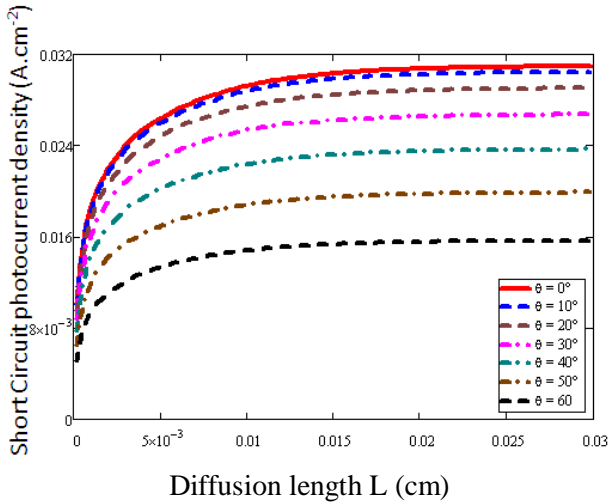


Figure 4: Profile of Short Circuit photocurrent density versus diffusion length for different incident angle values, $H = 0.03 \text{ cm}$, $S_f = 6.10^6 \text{ cm.s}^{-1}$

Figure 4 shows that for each incident angle, the short circuit photocurrent density increases, and is constant for high diffusion length values.

II.2 Effective diffusion length determination

The method used the calibrated short circuit photocurrent density and the experimental one J_{sc_exp} plots versus the diffusion length while the incident angle value is constant. We obtain the value of the effective minority carrier's diffusion length when the experimental short circuit current density J_{sc_exp} intercepts with the calibrated function $J_{sc}(L)$ (Figure 5) [15]. Then for each incident angle, the effective diffusion length is then extracted.

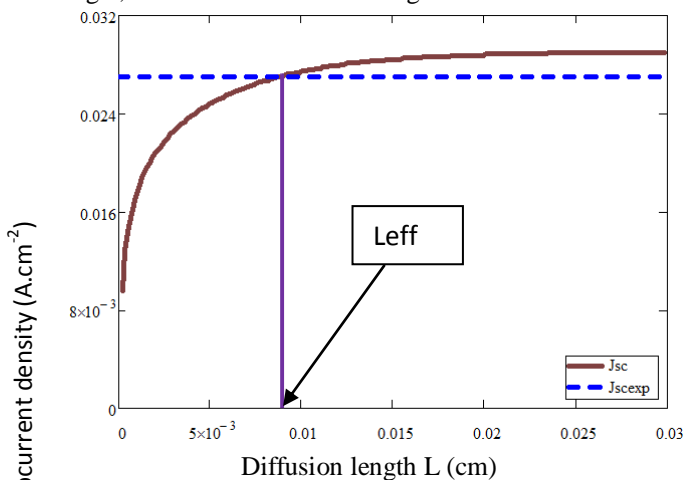


Figure 5: Determination of effective diffusion length, $H = 0.03 \text{ cm}$, $S_f = 6.10^6 \text{ cm.s}^{-1}$

II.3 The junction intrinsic recombination velocity:

Figure 6 represents the evolution of the current density as a function of the base recombination velocity for different incident angle values.

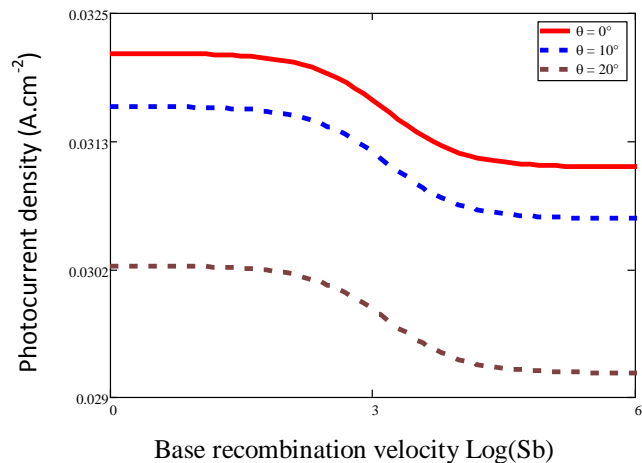


Figure 6: variation of the photocurrent density versus base recombination velocity
 $L=0.02 \text{ cm}$, $S_f = 6.10^6 \text{ cm.s}^{-1}$

The following curve (Figure 6) shows the variation of the photocurrent density versus base recombination velocity for different incident angle values. The photocurrent density is a decreasing function of the base recombination velocity. Either the photocurrent density decreases for high values of incident angle θ .

For a given operating point, there is a slight variation of the current density as a function of base recombination velocity.

We obtain greater values of photocurrent density for low Sb values: it is the case of backfield solar cells (BSF). For large Sb values, the photocurrent density is less important: it is the conventional case of ohmic solar cells [16].

As the photocurrent density J_{ph} remains constant for certain Sb values, we can write:

$$\left[\frac{\partial J_{ph}}{\partial Sb} \right] = 0 \quad (13)$$

From this equation, we then extract the expression of the junction recombination velocity depending only to the diffusion length.

$$Sf(L) = \frac{D}{L} \sum_{i=1}^3 \frac{b_i \cdot e^{-b_i \cdot H} + \frac{1}{L} \cdot \sinh\left(\frac{H}{L}\right) - b_i \cdot \cosh\left(\frac{H}{L}\right)}{\frac{1}{L} \cdot e^{-b_i \cdot H} + \left(b_i \cdot \sinh\left(\frac{H}{L}\right) - \frac{1}{L} \cdot \cosh\left(\frac{H}{L}\right) \right)} \quad (14)$$

Replacing the diffusion length L by $Leff$, we obtain $Sf(Leff) = Sf_0$ (15)

EXPERIMENTAL STUDY

Figure 7 present the experimental set up [8].



Figure 6: Experimental device for acquisition

For $\theta = 20^\circ$, we obtained the following curve with the analog oscilloscope (Figure 8).

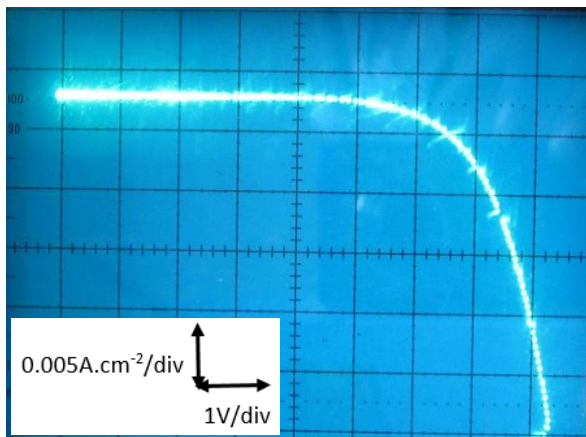


Figure 8: I-V Characteristic for $\theta = 20^\circ$
 From the I-V characteristic we can extract the experimental short-circuit photocurrent density.

III. EXPERIMENTAL RESULTS

The table below shows the results obtained from the experimental set up for an automatic characterization of the solar cell under several incident angle values. This table shows for each value of θ , the density of short circuit current, the effective diffusion length, the base recombination velocity and the intrinsic recombination velocity.

Table 2: Recombination parameters

θ ($^\circ$)	0	10	20	30	40	50	60
J_{sc_exp} ($10^{-3} A.cm^{-2}$)	28.5	28	27	25	22.5	19	15
L_{eff} (μm)	83.7	85.6	89.4	93.2	106.5	112.2	110
S_b ($10^3 cm/s$)	9.361	9.159	8.781	8.436	7.436	7.086	6.875
S_{f0} ($10^3 cm/s$)	2.026	2.026	2.026	2.025	2.024	2.024	2.023

On the above table, it should be noted that when the incident angle θ increases, the J_{sc_exp} decreases, and the carrier diffusion length increases. This means that for

high incident angle, the solar cell is exposed to bad lighting conditions.

CONCLUSION

The method proposed in this work considers the solar cell under a real operating condition. By help of the phenomenological parameters such as bulk and surface recombination velocity, the behaviour of an illuminated cell can be well described through the photocurrent, for all incident angles.

From calibrated photocurrent density as a function of diffusion length. We have extended the technics for bulk and surface recombination velocity determination in a silicon solar cell since the experimental short circuit current for each incident angle is known.

REFERENCES

- [1] Y. L. B. Bocande, A. Corr ea , M. L. Sow , G. Sissoko. "Bulk and surfaces parameters determination in high efficiency Silicon solar cells. Renewable Energy", vol 5, part III, pp. 1698-1700, 1994.
- [2] Th. Flohr and R. Helbig. Determination of minority-carrier lifetime and surface recombination velocity by Optical-Beam-Induced-Current measurements at different light wavelengths, J. Appl. Phys. Vol.66 (7), (1989) pp 3060 – 3065.
- [3] H. L. Diallo, A. Wereme, A. S. Maiga et G. Sissoko, "New approach of both junction and back surface recombination velocities in a 3D modelling study of a polycrystalline silicon solar cell", Eur. Phys. J. Appl. Phys. 42, pp.203–211, 2008.
- [4] F. Ahmed et S. Garg, "Simultaneous determination of diffusion length, lifetime and diffusion constant of minority carrier using a modulated beam", International Atomic Energy Agency, International centre for theoretical physics, Internal report IC 86, pp.129-134, 1987.
- [5] I. Gaye, R. Sam, A. D. Ser e, I. F. Barro, M. A. Ould El Moujtaba, R. Man e et G. Sissoko, "Effect of irradiation on the transient response of a silicon solar cell", International Journal of Emerging Trends and Technology in Computer Science, Volume 1, Issue 3, September – October, ISSN 2278-6856, pp. 210-214, 2012.
- [6] A. Thiam, M. Zoungrana, H. Ly Diallo, A Diao, N. Thiam, S. Gueye, M.M. Deme, M. Sarr et G. Sissoko, "Influence of Incident Illumination Angle on Capacitance of a Silicon Solar Cell under Frequency Modulation", Res. J. Appl. Sci. Eng. Technol. 5(04), pp. 1123-1128, 2012.
- [7] S. Mbodji, B. Mbow, F. I. Barro et G. Sissoko, "A 3D model for thickness diffusion capacitance of emitter-base junction determination in a bifacial

- polycrystalline solar cell under real operating condition”, Turk. J. Phys., vol. 35, pp. 281-291, 2011.
- [8] O. Sow, D. Diarisso, N. Z. A. MBodji, M. S. Diallo, A. Diao, I. Gaye, F. I. Barro, G. Sissoko. “*Experimental Device for Acquisition of Properties I-V and V(T) of the Solar By Automatic Change Operating Point*”. International Journal of Innovative Technology and Exploring Engineering (IJITEE), Volume-2, Issue-4, pp 330-334 March 2013.
- [9] F. I. Barro, A. S. Maiga, A. Wereme et G. Sissoko, “*Determination of recombination parameters in the base of a bifacial silicon solar cell under constant multispectral light*”, Phys. Chem. News 56, pp.76-84, 2010.
- [10] T. Flohr et R. Helbig, “*Determination of minority-carrier lifetime and surface recombination velocity by Optical-Beam-Induced-Current measurements at different light wavelengths*”, J. Appl. Phys. Vol.66 (7), pp. 3060 – 3065, 1989.
- [11] S. R. Wenham, M.A. Green, M. E. Watt et R. Corkish, “*Applied Photovoltaics*”, 2nd edition, ARC Centre for Advanced Silicon Photovoltaics and Photonics, 2007.
- [12] H. Mathieu et H. Fanet, “*Physique des semiconducteurs et des composants électroniques*”, 6ème Ed, Dunod, 2009.
- [13] J. L. Balenzategui et F. Chenlo, “*Measurement and analysis of angular response of bare and encapsulated silicon solar cells*” Sol. Energy Mater. Sol, 86 pp.53–83, 2005.
- [14] L. Bousse, L. S. Mostarshed, D. Hafeman, M. Sartore, M. Adami and C. Nicolini, “*Investigation of carrier transport through silicon wafers by photocurrent measurements*”, J. Appl. Phys. Vol.75, (8), pp. 4000 – 4008, 1994.
- [15] K. Taniguchi, “*Graphical technique to determine minority carrier lifetime and surface generation velocity using triangular-voltage sweep C-V method*”, Solid-State Electronics, Volume 21, Issue 8, pp. 1057-1061, 1978.
- [16] H. Ly Diallo, B. Dieng, I. Ly, M.M. Dione, M. Ndiaye, O.H. Lemrabott, Z.N. Bako, A. Wereme and G. Sissoko “*Determination of the Recombination and Electrical Parameters of a Vertical Multijunction Silicon Solar Cell*”, Research Journal of Applied Sciences, Engineering and Technology 4(16): 2626-2631, 2012